

The $\text{N}_2\text{O}\cdot\text{N}_2\text{O}$, $\text{N}_2\text{O}\cdot\text{SO}_2$, and $(\text{N}_2\text{O})_2\cdot\text{SO}_2$ van der Waals Complexes: An ab Initio Theoretical Analysis

H. Valdés and J. A. Sordo*

Laboratorio de Química Computacional, Departamento de Química Física y Analítica, Facultad de Química, Universidad de Oviedo, Julián Clavería 8, 33006, Oviedo, Principado de Asturias, Spain.

Received: September 18, 2003; In Final Form: January 16, 2004

The potential energy surfaces of the $\text{N}_2\text{O}\cdot\text{SO}_2$, $\text{N}_2\text{O}\cdot\text{N}_2\text{O}$, and $(\text{N}_2\text{O})_2\cdot\text{SO}_2$ van der Waals systems were extensively explored at the MP2 level of theory using Pople's 6-31G(d,p) and Dunning's cc-pVDZ, aug-cc-pVDZ, and cc-pVTZ basis sets. A total of 19 structures (seven for the trimer and six for each dimer) corresponding to stationary points on the potential energy surfaces were located and characterized. A dynamic structure corresponding to the interconversion of a number of configurations, which are of similar geometries and close in energy, is proposed for the $\text{N}_2\text{O}\cdot\text{SO}_2$ dimer. It is consistent with the asymmetric structure derived from microwave spectroscopic studies and explains the splitting of the rotational bands experimentally observed. The slipped-parallel configuration theoretically predicted for the $\text{N}_2\text{O}\cdot\text{N}_2\text{O}$ structure agrees with the geometry derived from infrared spectroscopy. One of the lower energy configurations predicted by ab initio methodologies for the $(\text{N}_2\text{O})_2\cdot\text{SO}_2$ trimer structure agrees rather well with that derived from Fourier transform microwave spectroscopy. Symmetry-adapted perturbation theory throws light into the physically meaningful contributions to the interaction energy and helped us to rationalize the trimer geometry in terms of dimer interactions present in the isolated dimers located on the ab initio potential energy surfaces, most of them experimentally undetected.

1. Introduction

Impressive advances in the development of modern spectroscopic techniques,^{1,2} particularly high-resolution Fourier transform microwave spectroscopy coupled to a supersonic gas expansion,³ have made possible the structural determination of a great variety of weakly bound complexes including donor–acceptor, hydrogen-bonded, and van der Waals dimer systems.^{4–7} Parallel developments in computer technology and electronic structure theory^{8,9} helped to complement such experimental works throwing additional light upon the nature of the interactions responsible for the formation of molecular associations.¹⁰

Studies on larger size clusters are desirable because they would provide valuable insights into the process of passing from the gas phase to condensed matter. However, the extension of high-resolution spectroscopic methods to the study of trimers and larger size clusters becomes more and more complicated, especially for systems involving nonlinear molecules, one of the main difficulties being the choice of suitable structures to start with the spectroscopic analysis.¹¹ Theoretical calculations represent a very powerful tool to make structural and energetic predictions available to experimentalists in order to help them to assign spectra.

On the other hand, theoretical analysis allows one to gain insight into the nature of the interactions responsible for the cluster formation, thus becoming a useful, as well as necessary, complement to the experimental work. Calculations based on semiempirical potentials have proven useful in the study of molecular associations.^{12,13} However, there are reasons supporting the preference for the use of ab initio methodologies.^{14,15} Among them, perhaps the most important one is the possibility offered by ab initio methods of improving, in a systematic way,

the results (structural, energetic, dynamical) for the systems under study, with the only limitation being the computer capabilities (software and hardware) available.

In recent publications, Peebles and Kuczkowski reported the structures of $\text{N}_2\text{O}\cdot\text{SO}_2$ dimer¹⁶ and $(\text{N}_2\text{O})_2\cdot\text{SO}_2$ trimer,¹⁷ both obtained from Fourier transform microwave spectroscopy. The latter represents the first trimer containing a bent molecule to be studied by microwave spectroscopy. These authors showed that the ORIENT program,¹⁸ which employs a semiempirical potential including electrostatic, dispersion, and repulsion terms, was a useful tool in the assignment of the spectra in the case of the trimer structure. For the $\text{N}_2\text{O}\cdot\text{SO}_2$ dimer, however, ORIENT modeling using default parameters has given poor agreement with experiment.¹⁷

As a part of a project which contemplates the systematic study of trimer structures,^{19–24} we decided to apply ab initio methodologies in the study of the $\text{N}_2\text{O}\cdot\text{SO}_2$ and $\text{N}_2\text{O}\cdot\text{N}_2\text{O}$ dimers and the $(\text{N}_2\text{O})_2\cdot\text{SO}_2$ trimer. Our goal is 4-fold: (a) to assess the suitability of the ab initio methodology to study trimer systems by comparing the theoretical predictions with the experimental data, (b) to compare ab initio predictions with ORIENT semiempirical results, (c) to apply ab initio methods based on perturbative treatments in the calculation of the physically meaningful contributions to the interaction energy for the different conformations, and (d) to interpret the formation of the trimer structure in terms of the relative orientation of the dimer faces, taking as a reference the isolated dimer structures. The two later points are particularly relevant in order to throw light upon the process of the formation of condensed phases.

2. Methods

The potential energy surfaces (PESs) of the $\text{N}_2\text{O}\cdot\text{SO}_2$, $\text{N}_2\text{O}\cdot\text{N}_2\text{O}$, and $(\text{N}_2\text{O})_2\cdot\text{SO}_2$ van der Waals systems were extensively analyzed at the MP2 level of theory²⁵ using Pople's 6-31G(d,p)²⁵

* Author to whom correspondence should be addressed. Fax: +34985237850. E-mail: jasn@correo.uniovi.es.

and Dunning's cc-pVDZ, aug-cc-pVDZ, cc-pVTZ^{26,27} basis sets. Our previous works on similar systems showed that MP2 geometry predictions with these basis sets are quite reasonable. Further MP4SDTQ//MP2 and QCISD(T)//MP2 calculations were carried out to improve the energy predictions. It is well-known²⁸ that the QCISD(T) level provides energy predictions quite similar to the ones obtained with the CCSD(T) method, and this latter level has been shown to reproduce quite well, in general, the CCSDT energetic results.^{29–32} Therefore, the QCISD(T)//MP2 energies reported in this work should be reliable.

To circumvent problems associated with the basis set superposition error (BSSE) in the supermolecule calculations,³³ two different approaches were adopted: (a) the original counterpoise procedure (CP) proposed by Boys and Bernardi³³ and (b) extrapolations to the complete basis set (CBS)^{29,31} by exploiting the regular behavior observed by the energies obtained with MP2/cc-pVXZ (X = D, T, Q) series of correlation-consistent basis sets.²⁹

All the stationary points located on the N₂O·SO₂, N₂O·N₂O, and (N₂O)₂·SO₂ PESs were characterized as minima, transition structures, or higher-order saddle points by computing the Hessian matrix and obtaining the corresponding eigenvalues. Further characterization of the interactions responsible for the formation of the trimers was carried out by performing a Bader topological analysis of the charge densities.³⁴

Ab initio many-body symmetry-adapted perturbation theory (SAPT) calculations³⁵ were carried out on the different dimer and trimer structures in order to determine the contributions arising from the physically meaningful forces (electrostatic, induction, dispersion, and exchange) to the total interaction energy.

In the SAPT formalism, the interaction energy, $E_{\text{int}}(\text{SAPT})$, is calculated as

$$E_{\text{int}}(\text{SAPT}) = E_{\text{int}}^{\text{HF}} + E_{\text{int}}^{\text{CORR}} \quad (1)$$

where $E_{\text{int}}^{\text{HF}}$ represents the supermolecular Hartree–Fock (HF) interaction energy

$$E_{\text{int}}^{\text{HF}} = E_{\text{pol}}^{(10)} + E_{\text{exch}}^{(10)} + E_{\text{ind,r}}^{(20)} + E_{\text{exch-ind,r}}^{(20)} + \delta E_{\text{int}}^{\text{HF}} \quad (2)$$

with $\delta E_{\text{int}}^{\text{HF}}$ collecting all higher-order induction and exchange corrections contained in $E_{\text{int}}^{\text{HF}}$ and not computed by the SAPT code (r indicates that the corresponding term was computed with the inclusion of the coupled HF response of the perturbed system).³⁶

$E_{\text{int}}^{\text{CORR}}$ contains the correlated portion of the interaction energy approximated by SAPT as

$$E_{\text{int}}^{\text{CORR}} = E_{\text{pol,r}}^{(12)} + E_{\text{exch}}^{(11)} + E_{\text{exch}}^{(12)} + {}^t E_{\text{ind}}^{(22)} + {}^t E_{\text{exch-ind}}^{(22)} + E_{\text{disp}}^{(20)} + E_{\text{exch-disp}}^{(20)} \quad (3)$$

where the t superscript indicates that the true correlation effects,³⁶ which represent those parts of the $E_{\text{ind}}^{(22)}$ energy that are not included in the term $E_{\text{ind,r}}^{(20)}$ in eq 2, are collected.

The relaxation energy (E_{RELAX}) is defined as

$$E_{\text{RELAX}} = D_e - E_{\text{int}}^{\text{SUP}} \quad (4)$$

where D_e is the stabilization energy and $E_{\text{int}}^{\text{SUP}}$ the supermolecule interaction energy.

It can be shown³⁷ that the results obtained in eq 1 for $E_{\text{int}}(\text{SAPT})$, using eqs 2 and 3, tend asymptotically to the values which would be predicted at the supermolecule MP2 level.

Given the important role which is expected to be played by the dispersion contributions in the weakly bound systems under study (see below), the SAPT calculations reported in this work have been performed using Dunning's aug-cc-pVDZ basis set which includes diffuse functions.³⁸

3. Results and Discussion

3.1. Geometries and Energetics. Seven minimum energy structures (**I–VII**) were located and characterized on the (N₂O)₂·SO₂ PES. Figure 1 shows two views of each, Table 1 collects the most representative geometrical parameters, and Table 2 contains the corresponding rotational constants and dipole moments as computed at the MP2/cc-pVTZ level. All the structures were further characterized by analyzing the electronic density. The characteristics of the critical points³⁴ located are available as Supporting Information. Three intermolecular bond critical points associated with the interactions between the dimers into the trimer were located. A ring critical point was also found for each structure. The characteristic set of the seven structures **I–VII**, (9,9,1,0) (nine nuclei, nine bond paths, one ring, and no cages) fulfils the Poincaré–Hopf relationship.³⁴ This topological analysis is fully consistent with a trimer cluster structure.

In structures **I–III**, the SO₂ is oriented so that its oxygens are straddling one of the N₂O units. The two N₂O monomers adopt a relative orientation which is intermediate between T-shaped and crossed structures. **I** and **II** differ from each other basically in the orientation of the N₆–N₅–O₇ monomer (see Figure 1 for notation). Whereas in **I** O₇ points toward the oxygen atom of the second N₂O monomer (O₃), in structure **II** it is N₆ which points toward O₃. In the case of structures **I** and **III**, the main difference refers to the orientation of the N₂–N₁–O₃ monomer as shown in Figure 1.

Structures **IV–VII** are triangular configurations in which the two N₂O monomers adopt slightly slipped-parallel geometrical dispositions. The N₂O monomers show a parallel alignment in structures **IV–V**, and they differ from each other basically in the orientation chosen by the SO₂ monomer. Whereas in **IV** the oxygen atoms of SO₂ point toward the N₂–N₁–O₃ monomer, in **V** they point toward the N₆–N₅–O₇ monomer. In structures **VI** and **VII** the two N₂O monomers adopt an antiparallel alignment with structure **VII** being that in which the two oxygens are closer to each other.

Table 1 collects the 10 parameters chosen by Peebles and Kuczkowski¹⁷ to define the (N₂O)₂·SO₂ structure as computed for the seven minimum energy configurations characterized as minima at the MP2/cc-pVTZ level of theory. Table 2 contains the corresponding rotational constants and dipole moments. It is clear from inspection of Tables 1 and 2 that structure **I** corresponds to the experimental geometry derived from the microwave spectra.¹⁷ The discrepancy found between the measured dipole moment and the MP2/cc-pVTZ theoretical estimate, already observed in other van der Waals complexes,³⁹ should be ascribed to the well-known difficulties associated with the calculation of dipole moments.⁴⁰

Peebles and Kuczkowski reported¹⁷ that the equilibrium structure of **I** (the one predicted by ab initio calculations) is probably within ±0.05 Å and ±5° of the N₂O-related parameters in Table 1 (first seven rows), whereas the parameters associated with SO₂ (next three rows) are less certain, probably within ±10°. Bearing in mind this observation, we conclude that the MP2/cc-pVTZ geometry represents a very good prediction

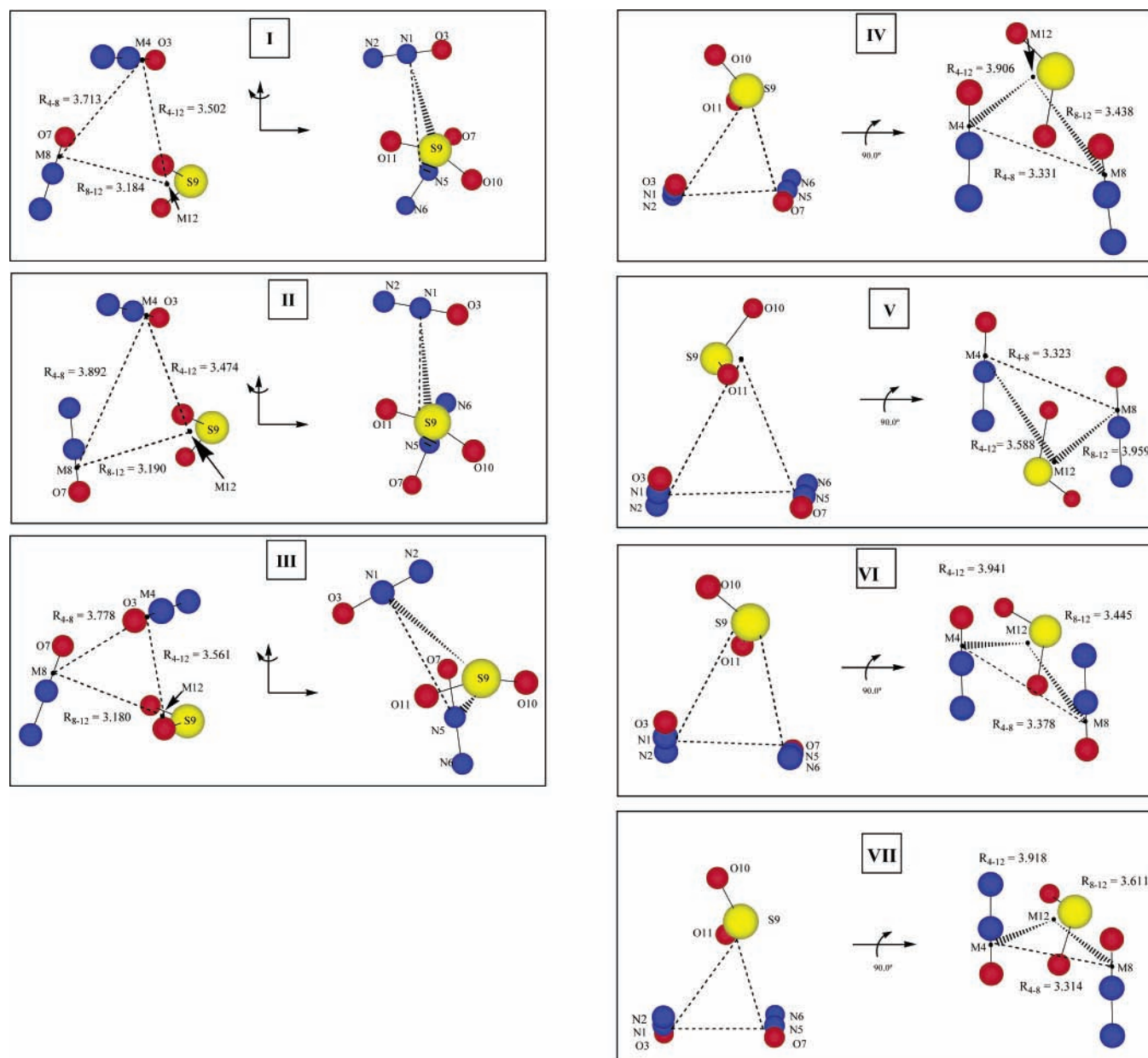


Figure 1. $(\text{N}_2\text{O})_2\cdot\text{SO}_2$ minimum energy structures **I–VII** as computed at the MP2/cc-pVTZ level of theory. Distances are given in angstroms and angles in degrees. Further structural parameters are given in Table 1 and as Supporting Information. The Ms stand for the corresponding centers of mass of the monomers.

TABLE 1: MP2/cc-pVTZ Structural Parameters for the Minimum Energy Structures I–VII Located on the $(\text{N}_2\text{O})_2\cdot\text{SO}_2$ PES^a

parameters	exptl ^b	structure						
		I	II	III	IV	V	VI	VII
$r(\text{M}_4\text{--M}_8)$	3.8558(23)	3.713	3.892	3.778	3.331	3.323	3.378	3.314
$r(\text{M}_4\text{--M}_{12})$	3.5316(13)	3.502	3.474	3.561	3.906	3.588	3.941	3.918
$\angle(\text{M}_{12}\text{--M}_4\text{--M}_8)$	52.494(26)	52.3	50.9	51.3	56.0	69.6	55.5	59.2
$\angle(\text{N}_1\text{--M}_4\text{--M}_8)$	83.330(85)	85.0	87.5	98.1	116.4	117.1	68.2	114.9
$\tau(\text{N}_1\text{--M}_4\text{--M}_8\text{--M}_{12})$	-129.99(10)	-126.9	128.8	-50.0	-98.6	-53.1	81.8	-97.8
$\angle(\text{N}_5\text{--M}_8\text{--M}_{12})$	97.672(95)	98.3	89.2	95.4	116.2	70.8	116.6	69.5
$\tau(\text{N}_5\text{--M}_8\text{--M}_{12}\text{--M}_4)$	-151.19(21)	-141.5	-25.6	148.0	-56.7	-77.9	-53.1	130.1
$\angle(\text{S}_9\text{--M}_{12}\text{--M}_4)$	90.75(14)	102.6	102.4	106.4	73.2	90.4	72.8	69.4
$\tau(\text{S}_9\text{--M}_{12}\text{--M}_4\text{--M}_8)$	163.83(84)	173.0	-175.5	-176.1	122.0	-63.9	121.1	104.5
$\tau(\text{O}_{10}\text{--S}_9\text{--M}_{12}\text{--M}_4)$	-118.66(36)	-122.0	117.9	119.3	-161.6	-125.4	-162.4	-176.9

^a Distances are given in angstroms and angles in degrees (see Figure 1 for notation). ^b See ref 17.

which confirms previous findings when studying similar systems that MP2 optimizations provide, in general, acceptable geometries for dimer and trimer van der Waals complexes.^{19–24}

As reported elsewhere,²⁴ because of the extreme flatness

exhibited by the PES of this type of system, relatively important geometrical variations may lead to insignificant energy changes. Thus, we detected some discrepancies for the geometries of structures **I–III** computed with the 6-31G(d,p), cc-pVDZ, and

TABLE 2: MP2/cc-pVTZ Rotational Constants (MHz) and Dipole Moments (debye) for the Minimum Energy Structures I–VII Located on the (N₂O)₂·SO₂ PES (See Figure 1 for Notation)

structure	A	B	C	μ
I	1398.2	1140.5	768.0	1.822
II	1420.6	1100.5	746.9	1.725
III	1407.4	1112.5	747.5	1.555
IV	1656.0	933.6	700.7	1.677
V	1646.8	892.6	675.9	1.312
VI	1644.8	920.9	690.9	1.440
VII	1633.6	905.0	677.7	1.525
exptl ^a	1369.1014(11)	1115.5816(11)	730.5790(4)	1.396(2)

^a See ref 17.

aug-cc-pVDZ basis sets when compared with the cc-pVTZ predictions (a complete list of the MP2 geometrical parameters for the seven structures I–VII as computed with all the basis sets employed is available as Supporting Information). For example, Table 3 shows that the double- ζ basis sets predictions for the distance between the centers of mass of the two N₂O monomers in structure I are much shorter than the experimental values and the cc-pVTZ prediction. However, the corresponding dissociation energies are quite similar. Let us focus on the MP2/aug-cc-pVDZ level in order to illustrate this point. Despite the rather short M₄–M₈ distance predicted at this level [see Table 3: 3.325 Å vs 3.713 Å (MP2/cc-pVTZ) or 3.8558(23) Å (experimental value)], the MP2/aug-cc-pVDZ dissociation energy of the MP2/cc-pVTZ geometry (MP2/aug-cc-pVDZ//MP2/cc-pVTZ) is 2107 cm⁻¹, to be compared with the dissociation energy of the MP2/aug-cc-pVDZ geometry (MP2/aug-cc-pVDZ//MP2/aug-cc-pVDZ) of 2173 cm⁻¹. Interestingly, the MP2/aug-cc-pVDZ geometry compares rather well with one of the structures located on the ORIENT semiempirical PES¹⁷ (see below). When appreciable discrepancies were detected, the MP2/cc-pVTZ geometries were chosen to carry out the SAPT calculations reported below.

Table 4 collects the dissociation energies computed at different levels of theory for the seven (N₂O)₂·SO₂ configurations. As a global conclusion, all the structures are very close in energy. We computed MP2/CBS extrapolations for the dissociation energies of structures I–III in order to assess the influence of the BSSE. The BSSE-free computed dissociation energies were 1566, 1624, and 1593 cm⁻¹, respectively, thus keeping the relative ordering obtained at the MP2/cc-pVTZ level.

There are several factors that should be taken into account to assess the reliability of the above energy predictions: (a) as shown in Table 4 the use of higher levels of theory (MP4SDTQ, QCISD(T), including the important contributions arising from the triple substitutions)^{8,9} is required to make more quantitative

energy predictions^{38,41} and (b) addition of diffuse functions to the cc-pVTZ basis sets is expected to play a significant role in order to make suitable predictions among the energetically close-lying structures I–VII.^{38,42–44} Thus, QCISD(T)/aug-cc-pVTZ//MP2/aug-cc-pVTZ calculations should be carried out in order to make a more quantitative discussion on the relative stabilities of structures I–VII. Unfortunately, such a level of theory (involving QCISD(T) calculations with 418 basis functions) is presently beyond most computer capabilities. It should be remarked at this point that this rather frustrating conclusion is a direct consequence of the fact that the MP2/aug-cc-pVDZ geometries are not appropriate for structures I–III. Otherwise, the more affordable QCISD(T)/aug-cc-pVDZ//MP2/aug-cc-pVDZ level has proven sufficient to reproduce both geometrical and energetic experimental data on van der Waals complexes (see refs 2, 19–24 and references therein).

To make a quantitative assessment of the role played by diffuse functions, we computed MP2/CBS extrapolations for the MP2/cc-pVTZ geometries of the I–III structures using aug-cc-pVXZ (X = D, T, Q) basis sets. The larger calculations involved 724 basis functions and required about 6 h of CPU time each running on the NEC-SX5 supercomputer (8 GB RAM) at the Centro Svizzero di Calcolo Scientifico (Manno, Switzerland). The resulting dissociation energies were 1675, 1723, and 1689 cm⁻¹, respectively. These values agree rather well with those estimated from the MP2/CBS extrapolations employing basis sets with no diffuse functions, namely, cc-pVXZ (X = D, T, Q) (1566, 1624, and 1593 cm⁻¹, respectively). These results do support the reliability of the level of theory adopted in the present work.

The semiempirical ORIENT potential predicts three minimum energy structures on the PES. The most stable one (–2285 cm⁻¹; see structure I in ref 17) strongly resembles both the experimentally observed and the ab initio MP2/cc-pVTZ predicted configuration I (see Table 1). The two remaining ORIENT structures (–2125 and –2107 cm⁻¹) have the N₂O molecules aligned roughly parallel to each other. One of them is very similar to the MP2/aug-cc-pVDZ geometry for structure I. The other one looks like the MP2 geometry predicted by all the basis sets for the structure IV. None of the energetically close-lying structures II and III are present on the ORIENT PES. Therefore, it seems that the ORIENT semiempirical potential is not able to provide a reliable representation of the ab initio PES, although it makes a rather good prediction on the experimentally observed structure.¹⁷

3.2. Nature of the Interactions in the (N₂O)₂·SO₂ Trimer Structures. One of the most important points in any research on cluster formation should be to analyze to what extent the geometries exhibited by larger size clusters are determined by energetically favored orientations of the monomers involved.

TABLE 3: MP2 Structural Parameters for the Minimum Energy Structure I Located on the (N₂O)₂·SO₂ PES^a

parameters	exptl ^b	structure I			
		6-31G(d,p)	cc-pVDZ	aug-cc-pVDZ	cc-pVTZ
R(M ₄ –M ₈)	3.8558(23)	3.567	3.689	3.325	3.713
R(M ₄ –M ₁₂)	3.5316(13)	3.499	3.515	3.512	3.502
∠(M ₁₂ –M ₄ –M ₈)	52.494(26)	53.6	51.4	57.6	52.3
∠(N ₁ –M ₄ –M ₈)	83.330(85)	83.2	86.7	74.6	85.0
τ(N ₁ –M ₄ –M ₈ –M ₁₂)	–129.99(10)	–127.7	–127.6	–131.1	–126.9
∠(N ₅ –M ₈ –M ₁₂)	97.672(95)	102.6	97.8	111.5	98.3
τ(N ₅ –M ₈ –M ₁₂ –M ₄)	–151.19(21)	–132.7	–141.7	–116.5	–141.5
∠(S ₉ –M ₁₂ –M ₄)	90.75(14)	100.6	107.8	85.6	102.6
τ(S ₉ –M ₁₂ –M ₄ –M ₈)	163.83(84)	172.7	176.4	163.9	173.0
τ(O ₁₀ –S ₉ –M ₁₂ –M ₄)	–118.66(36)	–125.3	–123.2	–130.9	–122.0

^a Distances are given in angstroms and angles in degrees (see Figure 1 for notation). ^b See ref 17.

TABLE 4: Dissociation Energies (kcal·mol⁻¹/cm⁻¹) for the Minimum Energy Structures I–VII Located on the (N₂O)₂·SO₂ PES as Computed at Different Levels of Theory (See Figure 1 for Notation)

basis	method		
	MP2	MP4SDTQ ^a	QCISD(T) ^a
Structure I			
6-31G(d,p)	5.4/1870	5.0/1732	5.3/1863
cc-pVDZ	4.8/1675	4.4/1531	4.8/1677
aug-cc-pVDZ ^b	6.2/2173	6.4/2217	6.0/2093
cc-pVTZ ^b	5.0/1742		
Structure II			
6-31G(d,p)	5.0/1754	4.8/1666	4.1/1426
cc-pVDZ	4.6/1604	4.3/1509	3.7/1296
aug-cc-pVDZ ^b	6.2/2164	6.3/2202	5.0/1737
cc-pVTZ ^b	5.1/1785		
Structure III			
6-31G(d,p)	5.3/1866	5.0/1775	4.7/1649
cc-pVDZ	5.0/1745	4.8/1660	4.2/1443
aug-cc-pVDZ ^b	6.3/2186	6.5/2272	5.6/1929
cc-pVTZ ^b	5.1/1776		
Structure IV			
6-31G(d,p)	5.1/1781	4.8/1674	5.0/1752
cc-pVDZ	4.3/1525	4.0/1417	4.4/1539
aug-cc-pVDZ ^b	6.0/2097	6.1/2132	5.8/2045
cc-pVTZ ^b	4.5/1585		
Structure V			
6-31G(d,p)	5.2/1795	5.4/1860	3.4/1164
cc-pVDZ	4.8/1682	5.1/1758	3.0/1047
aug-cc-pVDZ ^b	6.3/2186		
cc-pVTZ ^b	4.7/1644		
Structure VI			
6-31G(d,p)	5.0/1735	4.8/1696	3.7/1298
cc-pVDZ	4.5/1575	4.4/1533	3.4/1196
aug-cc-pVDZ ^b	6.0/2113	6.2/2187	4.8/1697
cc-pVTZ ^b	4.5/1583		
Structure VII			
6-31G(d,p)	5.0/1749	4.7/1646	4.6/1592
cc-pVDZ	4.4/1524	4.1/1436	4.0/1388
aug-cc-pVDZ ^b	6.0/2079	6.1/2137	5.4/1876
cc-pVTZ ^b	4.5/1559		

^a MP4SDTQ//MP2 and QCISD(T)//MP2 single-point calculations.^b Zero-point energy estimated at the MP2/cc-pVDZ level.

Such information can be of great interest in order to make geometry predictions on larger size clusters and, finally, on the condensed phase. In the present case, we will analyze whether a relation between the trimer faces of (N₂O)₂·SO₂ and the isolated dimers N₂O·SO₂ and N₂O·N₂O exists.

3.2.1. The N₂O·SO₂ and N₂O·N₂O Dimers. Tables 5 and 6 collect the twelve stationary points located on the PESs for the N₂O·SO₂ and N₂O·N₂O dimers as computed at the MP2 level of theory using the larger basis sets aug-cc-pVDZ and cc-pVTZ.

In the case of N₂O·SO₂ we located and characterized six stationary points on the PES (see Table 5). The structures denoted as **a–e** correspond to configurations in which the SO₂ straddles the N₂O molecule either symmetrically (**a**, C_s symmetry) or asymmetrically (**b–e**, C₁ symmetry). Structure **f** is a C_s configuration in which one of the two SO bonds roughly parallels the N₂O unit. Analysis of the Hessian matrix shows that **a** and **c** are minima and structure **b** presents one imaginary frequency (7–16 cm⁻¹, depending on the basis set used) at all levels of theory. Structure **d** is a minimum according to the aug-cc-pVDZ and cc-pVTZ basis sets and a transition structure according to cc-pVDZ (imaginary frequency, 10 cm⁻¹). It is not a stationary point on the MP2/6-31G(d,p) PES. Structures **e** and **f** are predicted to be minima with all basis sets but cc-pVTZ which predicts these structures to be transition structures

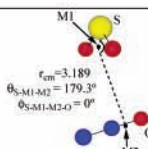
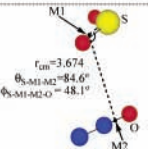
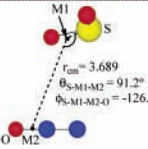
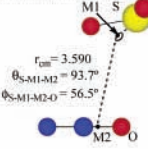
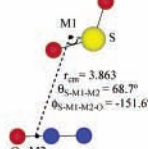
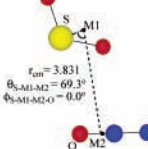
(both with imaginary frequencies of 7 cm⁻¹). It should be stressed at this point that, bearing in mind numerical accuracy, it is really unsafe to classify these stationary points as minima or transition structures. Indeed, Young⁴⁵ suggested that structures with frequencies in the range from -20 to +20 cm⁻¹ cannot be safely characterized. Schaefer and co-workers have insisted recently on this point.⁴⁶ On the other hand, all the structures are very close in energy (see Table 4) which clearly suggests that the potential energy surface is quite flat and many local minima can exist in close relation with the concept of cluster nonrigidity.¹² In agreement with Sun and Bernstein, one should no longer think of a van der Waals cluster like this as a rigid entity with a well-defined structure but as a dynamic system for which the structure is best considered an averaged attribute.¹² This is an important point that allows us to rationalize the experimental data obtained for the N₂O·SO₂ dimer from microwave spectroscopic studies. Peebles and Kuczkowski¹⁶ concluded that the N₂O·SO₂ structure lacks a symmetry plane, and a tunneling motion, attributed to an interconversion between mirror-image conformations through a C_s structure, splits the transitions into doublets. Our ab initio exploration of the PES suggests that the dynamic picture of the N₂O·SO₂ dimer corresponds to a shuttling motion of the SO₂ monomer around the N₂O axis as shown in Scheme 1.

As the nature of the stationary points cannot be unambiguously determined according to the discussion above, we are unable to propose an energy profile (maybe some stationary point in Scheme 1 is missing because of the difficulties associated with the location of minima and transition structures on very flat PESs), but the dynamic definition of the N₂O·SO₂ dimer by means of Scheme 1 allows for the rationalization of all the experimental facts.

ORIENT predicts for the N₂O·SO₂ dimer a totally asymmetric structure with one of the S–O bonds nearly parallel to the N–N–O axis.^{16,17} This semiempirical structure is quite similar to the N₂O·SO₂ (**b**) and N₂O·SO₂ (**d**) ab initio configurations. A C_s structure was characterized on the ORIENT PES as a transition structure. Therefore, the semiempirical predictions are also consistent with the dynamic definition of the N₂O·SO₂ structure proposed in Scheme 1.

For the N₂O·N₂O dimer, six stationary points were located on the PES (see Table 6). The structures denoted as **α–γ** are slipped-parallel configurations and were characterized as minima at all levels of theory. The structures **δ** and **ε** are quasi-T-shaped configurations and the structure **ζ** is a crossed configuration. One of the two quasi-T-shaped structures [N₂O·SO₂ (**δ**)] as well as the **ζ** crossed structure were characterized as transition structures exhibiting one imaginary frequency with all basis sets employed. They probably correspond to the transition structures connecting the slipped-parallel structures (unfortunately, this point cannot be confirmed as the algorithms available for connecting different structures on the PES do not work properly in the case of the very flat PESs corresponding to van der Waals systems).¹⁹ According to Table 6, the energy barrier involved is rather small. Ruoff et al.⁴⁷ reported that for energy barriers lower than about 400 cm⁻¹ a full conversion into the most stable structure should be expected. These results are consistent with the experimental observation that only a single isomer of the dimer is observed in the gas phase (the residual entropy observed in the crystal suggests that more than one isomer is present in the solid state).⁴⁸ The second T-shaped structure [N₂O·SO₂ (**ε**)] is a minimum on the PES for all the basis sets but aug-cc-pVDZ (for this latter basis set a very small imaginary frequency of 7 cm⁻¹ is predicted).

TABLE 5: Dissociation Energies in cm^{-1} (BSSE Values in Parentheses) for the Stationary Points Located on the $\text{N}_2\text{O}\cdot\text{SO}_2$ PES^b

	MP2	MP4SDTQ ^a	QCISD(T) ^a
$\text{N}_2\text{O}\cdot\text{SO}_2(\text{a})$ (C_s) 			
aug-cc-pVDZ	829 (506)	837 (491)	800 (461)
cc-pVTZ	763 (338)		
$\text{N}_2\text{O}\cdot\text{SO}_2(\text{b})$ (C_1) 			
aug-cc-pVDZ	640 (305)	639 (267)	743 (380)
cc-pVTZ	586 (313)		
$\text{N}_2\text{O}\cdot\text{SO}_2(\text{c})$ (C_1) 			
aug-cc-pVDZ	817 (465)	877 (483)	572 (184)
cc-pVTZ	637 (394)		
$\text{N}_2\text{O}\cdot\text{SO}_2(\text{d})$ (C_1) 			
aug-cc-pVDZ	750 (412)	748 (154)	855 (486)
cc-pVTZ	594 (326)		
$\text{N}_2\text{O}\cdot\text{SO}_2(\text{e})$ (C_1) 			
aug-cc-pVDZ	793 (421)	860 (454)	593 (195)
cc-pVTZ	625 (373)		
$\text{N}_2\text{O}\cdot\text{SO}_2(\text{f})$ (C_s) 			
aug-cc-pVDZ	739 (376)	741 (343)	839 (450)
cc-pVTZ	570 (298)		

^a MP4SDTQ//MP2 and QCISD(T)//MP2 single-point calculations. ^b Geometrical parameters are estimated at the MP2/cc-pVTZ level. M1 and M2 are the centers of mass of SO_2 and N_2O , respectively.

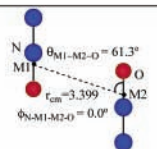
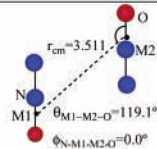
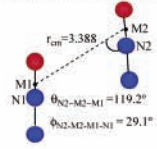
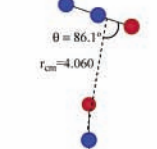
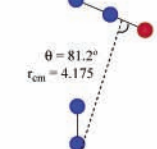
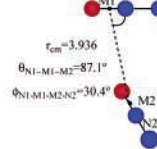
Although all the $\text{N}_2\text{O}\cdot\text{N}_2\text{O}$ dimers are energetically close-lying structures, the slipped-parallel structure $\text{N}_2\text{O}\cdot\text{SO}_2$ (α) is the one lowest in energy at the highest level of theory employed [QCISD(T)/aug-cc-pVDZ//MP2/aug-cc-pVDZ]. This theoretical prediction agrees with the fact that this configuration corresponds to the experimentally observed structure.⁴⁸ The need for rather high theoretical levels to properly estimate the dissociation energies of the different configurations has already been noted in the study of similar systems.⁴¹ No ORIENT semiempirical potential predictions for the $\text{N}_2\text{O}\cdot\text{N}_2\text{O}$ structure is reported by Peebles and Kuczowski.

3.2.2. *The $(\text{N}_2\text{O})_2\cdot\text{SO}_2$ Trimer.* Once we presented and analyzed in the previous section the structure of the isolated dimers, we are now ready to discuss the $(\text{N}_2\text{O})_2\cdot\text{SO}_2$ structure in terms of the dimer interactions.

Let us start with the experimentally detected structure **I** for $(\text{N}_2\text{O})_2\cdot\text{SO}_2$. Table 7 collects the SAPT contributions for three of the 12 stationary points located on the PESs of the $\text{N}_2\text{O}\cdot\text{SO}_2$ and $\text{N}_2\text{O}\cdot\text{N}_2\text{O}$ isolated dimers and for the dimer faces in structure **I**. Figure 2 depicts both the experimental and theoretical geometries for the isolated dimers together with those corresponding to the three dimer faces of the $(\text{N}_2\text{O})_2\cdot\text{SO}_2$ trimer structure **I**.

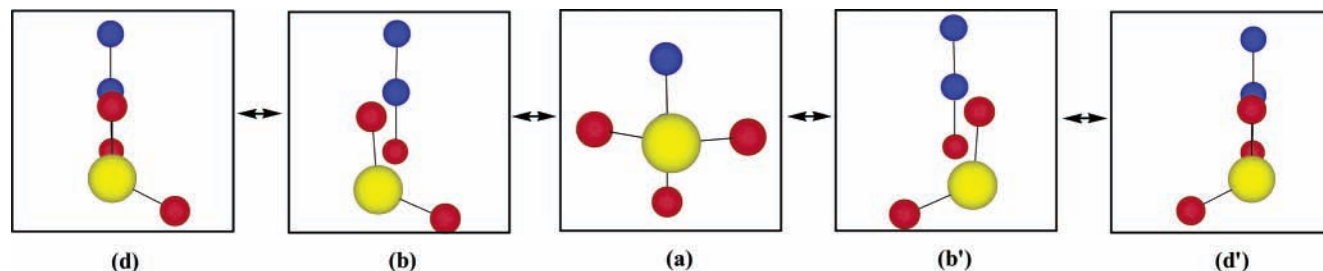
It is clear from Table 7 that all the dimer structures are van der Waals systems as the major contribution to the interaction energy comes from the dispersion forces. On the other hand, it is also noticeable that contributions arising from the induction forces are important. They are quite similar in magnitude to the electrostatic contributions. Furthermore, they vary appreciably when passing from one structure to another. Thus,

TABLE 6: Dissociation Energies in cm^{-1} (BSSE Values in Parentheses) for the Stationary Points Located on the $\text{N}_2\text{O}\cdot\text{N}_2\text{O}$ PES^b

	MP2	MP4SDTQ ^a	QCISD(T) ^a
 $\text{N}_2\text{O}\cdot\text{N}_2\text{O}$ (α) (C_s)	581 (345)	546 (287)	604 (352)
aug-cc-pVDZ cc-pVTZ	449 (240)		
 $\text{N}_2\text{O}\cdot\text{N}_2\text{O}$ (β) (C_s)	567 (311)	547 (270)	246 (-28)
aug-cc-pVDZ cc-pVTZ	439 (261)		
 $\text{N}_2\text{O}\cdot\text{N}_2\text{O}$ (γ) (C_s)	612 (365)	619 (351)	424 (161)
aug-cc-pVDZ cc-pVTZ	482 (285)		
 $\text{N}_2\text{O}\cdot\text{N}_2\text{O}$ (δ) (C_s)	439 (243)	428 (214)	376 (167)
aug-cc-pVDZ cc-pVTZ	341 (206)		
 $\text{N}_2\text{O}\cdot\text{N}_2\text{O}$ (ϵ) (C_s)	547 (313)	519 (266)	405 (156)
aug-cc-pVDZ cc-pVTZ	437 (288)		
 $\text{N}_2\text{O}\cdot\text{N}_2\text{O}$ (ζ) (C_1)	460 (281)	463 (267)	376 (185)
aug-cc-pVDZ cc-pVTZ	371 (223)		

^a MP4SDTQ//MP2 and QCISD(T)//MP2 single-point calculations. ^b Geometrical parameters are estimated at the MP2/cc-pVTZ level. M1 and M2 are the centers of mass of the two N_2O monomers.

SCHEME 1: Dynamic Definition of the $\text{N}_2\text{O}\cdot\text{SO}_2$ Dimer



for example, although the induction contribution to the interaction energy of $\text{N}_2\text{O}\cdot\text{SO}_2$ (**a**) (-616 cm^{-1}) is considerably smaller than the electrostatic part (-923 cm^{-1}), in the case of the $\text{N}_2\text{O}\cdot\text{SO}_2$ (**b**) structure, the induction forces make a contribution

(-810 cm^{-1}) even greater than the electrostatic forces (-808 cm^{-1}). All the above means that the induction forces must be taken into account in the studies of systems such as the ones considered in this work. Results arising from the application of

TABLE 7: SAPT/aug-cc-pVDZ//MP2/aug-cc-pVDZ Contributions (cm⁻¹) to the Interaction Energies for the N₂O·SO₂ and N₂O·N₂O Isolated Dimers and Dimer Faces in Structure I (See Tables 5 and 6 for Notation)^a

	isolated dimers			structure I ^b		
	N ₂ O·SO ₂ (a)	N ₂ O·SO ₂ (b)	N ₂ O·N ₂ O (ζ)	N ₂ O·SO ₂ (A)	N ₂ O·SO ₂ (B)	N ₂ O·N ₂ O
$E_{\text{pol}}^{(10)}$	-910	-1213	-335	-840	-1046	-342
$E_{\text{pol,r}}^{(12)}$	-13	405	16	-35	365	18
$E_{\text{pol}}^{(1)}$	-923	-808	-319	-875	-681	-324
$E_{\text{ind,r}}^{(20)}$	-444	-744	-183	-414	-593	-225
$\dagger E_{\text{ind}}^{(22)}$	-172	-66	-16	-157	-54	-17
$E_{\text{ind}}^{(2)}$	-616	-810	-199	-571	-647	-242
$E_{\text{disp}}^{(20)}$	-1167	-1154	-674	-1090	-1021	-646
$E_{\text{disp}}^{(2)}$	-1167	-1154	-674	-1090	-1021	-646
$E_{\text{exch}}^{(10)}$	1040	1288	546	959	1015	546
$E_{\text{exch}}^{(11)} + E_{\text{exch}}^{(12)}$	283	209	79	258	165	65
$E_{\text{exch}}^{(1)}$	1323	1497	625	1217	1180	611
$E_{\text{exch-ind,r}}^{(20)}$	381	560	150	358	436	191
$\dagger E_{\text{exch-ind}}^{(22)}$	147	50	13	136	40	14
$E_{\text{exch-disp}}^{(20)}$	106	120	50	97	95	52
$E_{\text{exch}}^{(2)}$	634	730	213	591	571	257
$\delta E_{\text{int}}^{\text{HF}}$	-34	-100	-24	-30	-68	-19
$E_{\text{int}}^{\text{HF}}$	34	-209	154	33	-256	151
$E_{\text{CORR}}^{\text{int}}$	-816	-438	-532	-790	-410	-513
$E_{\text{int}}(\text{SAPT})$	-783	-647	-378	-757	-666	-362
E_{RELAX}	15	4	0	23	26	35
$E_{\text{int}}^{\text{SUP}}(\text{NCP})$	-989	-866	-530	-956	-948	-443
$E_{\text{int}}^{\text{SUP}}(\text{CPR})$	-666	-532	-351	-651	-639	-274

^a The contributions for the rest of conformers are given as Supporting Information. ^b SAPT/aug-cc-pVDZ//MP2/cc-pVTZ calculations.

semiempirical models not including induction contributions should be considered with extreme caution.

Figure 2 shows that MP2/cc-pVTZ calculations predict that one of the N₂O·SO₂ faces in the (N₂O)₂·SO₂ trimer (the one denoted as **A** in Figure 2) strongly resembles the N₂O·SO₂ (**a**) isolated dimer structure in Table 5, in agreement with the experimental observation (see the experimental structures in Figure 2). SAPT calculations further support this fact as the different contributions to the interaction energy for the N₂O·SO₂ (**A**) face in the trimer are quite similar to the corresponding ones of the C_s N₂O·SO₂ (**a**) isolated dimer structure (see Table 7). The asymmetric structure N₂O·SO₂ (**A**) is slightly less stabilized by the attractive forces (electrostatic, induction, and dispersion), but at the same time, the repulsive exchange contributions are smaller.

In the case of the second N₂O·SO₂ face of the trimer (denoted as **B** in Figure 2), geometry predictions from ab initio calculations show that it resembles the N₂O·SO₂ (**b**) dimer structure in Table 5. Again, the SAPT analysis gives support to that observation. Indeed, the different contributions to the interaction energy are similar for the N₂O·SO₂ (**B**) and N₂O·SO₂ (**b**) structures (see Table 7). The smaller contributions of the stabilizing forces in the trimer face are compensated by the parallel reduction in the exchange forces.

Finally, the N₂O·N₂O face in the (N₂O)₂·SO₂ structure **I** strongly resembles the N₂O·N₂O (ζ) structure of the isolated dimer in Table 5. The SAPT calculations fully corroborate such an identification. The orientation of the two N₂O monomers relative to each other is intermediate between T-shaped and crossed structures. As mentioned above, this structure was characterized as a transition structure probably connecting slipped-parallel configurations. Therefore, the speculative interpretation proposed by Peebles and Kuczowski^{11,17} for a similar system, that an intermediate configuration in the tunneling process of the dimer is “trapped” in the trimer, might also be plausible in the present case.

Therefore, as in our previous studies on trimers,^{21–24} we have been able to rationalize the experimental geometry exhibited by the (N₂O)₂·SO₂ complex in terms of optimum dimer interactions. It should be stressed at this point that this interpretation would have not been possible by analyzing experimental data, as the N₂O·SO₂ (**b**) and N₂O·N₂O (ζ) dimer structures have not been experimentally detected. This is a relevant contribution emerging from the theoretical analysis.

A detailed analysis of the geometries of the faces in the trimers **II–VII** (figures similar to Figure 2 are available for the rest of the structures as Supporting Information) and the SAPT components of the interaction energies (see Table 7 and the Supporting Information) leads to the conclusion that the seven minimum energy structures **I–VII** are made up from dimer faces which most of the time resemble the configurations of the different isolated dimers located on the PES. Thus, the trimer structure can be denoted as (**a,b,ζ**) as its three faces are N₂O·SO₂ (**a**), N₂O·SO₂ (**b**), and N₂O·N₂O (ζ), respectively. The rest of structures **II–VII** can be classified as (**a,b,ζ'**), (**a,c,ζ**), (**d,f,γ**), (**e,c,γ**), (**d,e,β**), and (**c,f,α**), respectively. ζ' refers to a crossed structure, totally similar to ζ, where the terminal nitrogen atom of one N₂O unit points toward the second N₂O monomer (in ζ, it is the oxygen atom which points toward the second N₂O monomer). Although a structure like ζ' was not located on the N₂O·N₂O PES, the SAPT analysis shows that the energy contributions to the N₂O·N₂O faces in the trimers **I** and **II** are quite similar.

As mentioned in previous works on similar systems,^{21–24} theoretical explorations looking for the existence of stable dimer associations not necessarily observed in the spectroscopic studies can be helpful to rationalize the geometrical disposition observed for the corresponding trimers.

4. Conclusions

An extensive ab initio exploration of the potential energy surfaces of the N₂O·SO₂ and N₂O·N₂O dimers and the (N₂O)₂·SO₂ trimer carried out at the MP2 level using Pople's

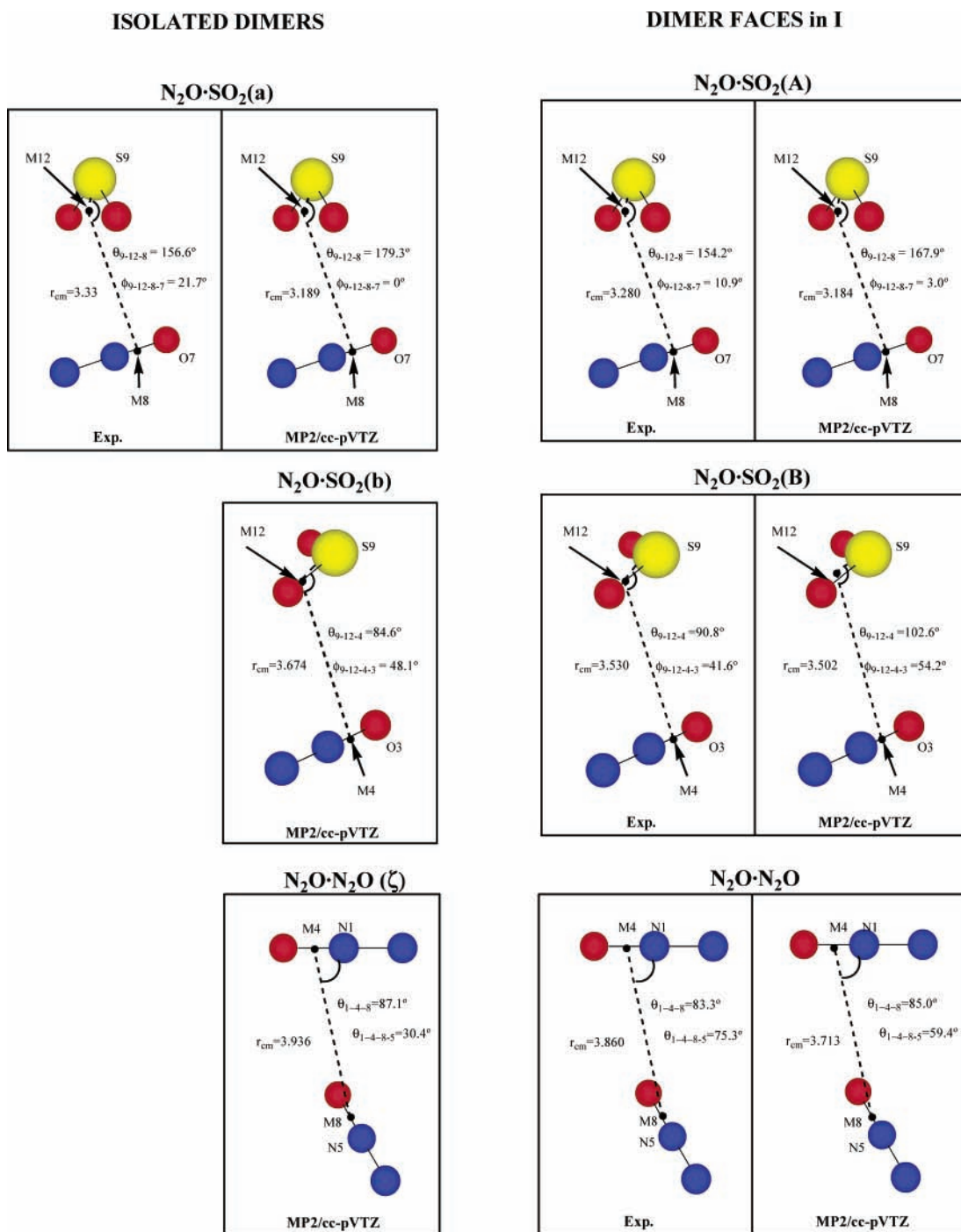


Figure 2. Experimental and MP2/cc-pVTZ geometries for the three dimer faces in the (N₂O)₂·SO₂ trimer I and their corresponding isolated dimers. Distances are given in angstroms and angles in degrees. The Ms stand for the corresponding centers of mass of the monomers.

6-31G(d,p) and Dunning's cc-pVDZ, aug-cc-pVDZ, and cc-pVTZ basis sets led to the location of 19 stationary points, six for each dimer and seven for the trimer. The imaginary frequencies of the saddle points are so small that the associated numerical inaccuracies make it impossible to carry out a definitive characterization of some such structures.

The presence of a number of structures geometrically similar and energetically close-lying in the case of the N₂O·SO₂ dimer suggests that the structure derived from the microwave spectra corresponds to an averaged structure representing the dynamical interconversion of several local minimum energy structures of similar geometries (cluster nonrigidity). This interpretation allows for the rationalization of the asymmetric character of the experimentally detected structure as well as for the observed

splitting of the transitions into doublets in the microwave spectrum of the N₂O·SO₂ dimer.

The lowest energy structure for the N₂O·N₂O dimer predicted by ab initio calculations is a slipped-parallel configuration with an antiparallel orientation of the two N₂O units, in agreement with sub-Doppler resolution infrared spectroscopic measurements.

One of the lower energy configurations for the (N₂O)₂·SO₂ trimer predicted by ab initio calculations compares rather well with the one derived from microwave spectroscopic studies. In this structure, the SO₂ is oriented so that its oxygens are straddling one of the N₂O molecules. The two N₂O monomers adopt a relative orientation which is intermediate between T-shaped and crossed structures.

ORIENT semiempirical potential predicts a smaller number of possible structures than ab initio methodologies do, and sometimes ($N_2O \cdot SO_2$ dimer) they differ considerably from the experimental geometries.

SAPT analyses suggest that dispersion forces are the most important ones in the stabilization of this type of van der Waals system. On the other hand, induction contributions are by no means negligible. Therefore, results arising from semiempirical potentials with no consideration of the induction forces should be handled with extreme care.

Examination of the geometrical parameters of the dimer faces in the $(N_2O)_2 \cdot SO_2$ trimers together with the SAPT analyses of the different contributions to the interaction energy allow for the rationalization of the trimer geometries in terms of the dimer interactions present in the isolated dimer structures located on the potential energy surfaces and most of the time not detected experimentally.

Supporting Information Available: Figures and tables of geometrical parameters, rotational constants, Bader's topological analysis, and SAPT additional information. This material is available free of charge via the Internet at <http://pubs.acs.org>.

References and Notes

- (1) Castleman, A. W., Jr.; Bowen, K. H., Jr. *J. Phys. Chem. A* **1996**, *100*, 12911.
- (2) *Chem. Rev.* **2000**, 3861–4264.
- (3) Balle, T. J.; Flygare, W. H. *Rev. Sci. Instrum.* **1981**, *52*, 33.
- (4) Hobza, P.; Zahradník, R. *Intermolecular Complexes. The Role of van der Waals Systems in Physical Chemistry and in Biodisciplines*; Academia: Prague, 1988.
- (5) Jeffrey, G. A. *An Introduction to Hydrogen Bonding*; Oxford University Press: New York, 1997.
- (6) Stone, A. J. *The Theory of Intermolecular Forces*; Clarendon Press: Oxford, U.K., 1997.
- (7) Desiraju, G. R.; Steiner, T. *The Weak Hydrogen Bond in Structural Chemistry and Biology*; Oxford University Press: Oxford, U.K., 2001.
- (8) Yarkony, D. R., Ed.; *Modern Electronic Structure Theory*, World Scientific: Singapore, 1995; Parts I and II.
- (9) Helgaker, T.; Jorgensen, P.; Olsen, J. *Molecular Electronic Structure Theory*; Wiley: Chichester, U.K., 2002.
- (10) Chalasinski, G.; Szczesniak, M. M. *Chem. Rev.* **2000**, *100*, 4227.
- (11) Peebles, S. A.; Kuczkowski, R. L. *J. Mol. Struct. (THEOCHEM)* **2000**, *500*, 391.
- (12) Sun, S.; Bernstein, E. R. *J. Phys. Chem. A* **1996**, *100*, 13348.
- (13) Dykstra, C. E. *J. Phys. Chem. A* **1995**, *99*, 11680.
- (14) Hobza, P.; Selzle, H. L.; Schlag, E. W. *Chem. Rev.* **1994**, *94*, 1767.
- (15) Müller-Dethlefs, K.; Hobza, P. *Chem. Rev.* **2000**, *100*, 143.
- (16) Peebles, R. A.; Kuczkowski, R. L. *J. Phys. Chem. A* **2000**, *104*, 4968.
- (17) Peebles, R. A.; Kuczkowski, R. L. *J. Chem. Phys.* **2000**, *112*, 8839.
- (18) Stone, A. J.; Dullweber, A.; Hodges, M. P.; Popelier, P. L. A.; Wales, D. J. *ORIENT: A Program for Studying Interactions between Molecules*, version 3.2; University of Cambridge: Cambridge, U.K., 1995.
- (19) Rayón, V. M.; Sordo, J. A. *J. Phys. Chem. A* **1997**, *101*, 7414.
- (20) Rayón, V. M.; Sordo, J. A. *J. Chem. Phys. Lett.* **2001**, *341*, 575.
- (21) Valdés, H.; Sordo, J. A. *J. Comput. Chem.* **2002**, *23*, 444.
- (22) Valdés, H.; Sordo, J. A. *J. Phys. Chem. A* **2002**, *106*, 3690.
- (23) Valdés, H.; Sordo, J. A. *J. Phys. Chem. A* **2003**, *107*, 899.
- (24) Valdés, H.; Sordo, J. A. *J. Phys. Chem. A* **2003**, *107*, 7845.
- (25) Hehre, W. J.; Radom, L.; Schleyer, P. v. R.; Pople, J. A. *Ab Initio Molecular Orbital Theory*; Wiley: New York, 1986.
- (26) Dunning, T. H., Jr. *J. Chem. Phys.* **1989**, *90*, 1007.
- (27) Kendall, R. A.; Dunning, T. H., Jr. *J. Chem. Phys.* **1992**, *96*, 6796.
- (28) Jensen, F. *Introduction to Computational Chemistry*; Wiley: Chichester, U.K., 1999.
- (29) Dunning, T. H., Jr. *J. Chem. Phys. A* **2000**, *104*, 9062.
- (30) Feller, D.; Sordo, J. A. *J. Chem. Phys.* **2000**, *112*, 5604.
- (31) Feller, D.; Sordo, J. A. *J. Chem. Phys.* **2000**, *113*, 485.
- (32) Sordo, J. A. *J. Chem. Phys.* **2001**, *114*, 1974.
- (33) Boys, S. F.; Bernardi, F. *Mol. Phys.* **1970**, *19*, 553.
- (34) Bader, R. F. W. *Atoms in Molecules. A Quantum Theory*; Oxford University Press: New York, 1990.
- (35) Jeziorski, B.; Moszynski, R.; Szalewicz, K. *Chem. Rev.* **1994**, *94*, 1887.
- (36) Bukowski, R.; Jankowski, P.; Jeziorski, B.; Jeziorski, M.; Kucharski, S. A.; Moszynski, R.; Rybak, S.; Szalewicz, K.; Williams, H. L.; Wormer, P. E. S. *SAPT96: An ab Initio Program for Many-Body Symmetry-Adapted Perturbation Theory Calculations of Intermolecular Interaction Energies*; University of Delaware and University of Warsaw, 1996.
- (37) Chalasinski, G.; Szczesniak, M. M. *Mol. Phys.* **1988**, *63*, 205.
- (38) Sponer, J.; Hobza, P. *J. Phys. Chem. A* **2000**, *104*, 4592.
- (39) Rayón, V. M.; Sordo, J. A. *J. Chem. Phys.* **1997**, *107*, 7912.
- (40) Johnson, B. G.; Gill, P. M. W.; Pople, J. A. *J. Chem. Phys.* **1993**, *98*, 5612.
- (41) Valdés, H.; Rayón, V. M.; Sordo, J. A. *Int. J. Quantum Chem.* **2001**, *84*, 78.
- (42) Rayón, V. M.; Sordo, J. A. *J. Chem. Phys.* **1999**, *110*, 377.
- (43) Braña, P.; Menéndez, B.; Fernández, T.; Sordo, J. A. *J. Phys. Chem. A* **2000**, *104*, 10842.
- (44) Braña, P.; Sordo, J. A. *J. Am. Chem. Soc.* **2001**, *123*, 10348.
- (45) Young, D. *Computational Chemistry. A Practical Guide for Applying Techniques to Real World Problems*; Wiley: New York, 2001.
- (46) Xie, Y.; Jang, J.-H.; King, R. B.; Schaefer, H. F., III. *Inorg. Chem.* **2003**, *42*, 5219.
- (47) Ruoff, R. S.; Klots, T. D.; Emilsson, T.; Gutowski, H. S. *J. Chem. Phys.* **1990**, *93*, 3142.
- (48) Huang, Z. S.; Miller, R. E. *J. Chem. Phys.* **1988**, *89*, 5408.